Evaluation of radioiodinated vesamicol analogs for sigma receptor imaging in tumor and radionuclide receptor therapy

doi: 10.1111/j.1349-7006.2009.01279.x

Cancer Science
The official journal of the Japanese Cancer Association

Evaluation of radioiodinated vesamicol analogs for sigma receptor imaging in tumor and radionuclide receptor therapy

Kazuma Ogawa,[1,2,5] Kazuhiro Shiba,[2] Nasima Akhter,[3] Mitsuyoshi Yoshimoto,[3] Kohshin Washiyama,[3] Seigo Kinuya,[3] Keiichi Kawai[3,4] and Hirofumi Mori[2]

[1]Graduate School of Natural Science and Technology, [2]Advanced Science Research Center, [3]Graduate School of Medical Sciences, Kanazawa University, Kanazawa; [4]Biomedical Imaging Research Center, University of Fukui, Fukui, Japan

(Received May 18, 2009/Revised June 30, 2009/Accepted June 30, 2009/Online publication July 31, 2009)

It has been reported that sigma receptors are highly expressed in a variety of human tumors. In this study, we selected (+)-2-[4-(4-iodophenyl)piperidino] cyclohexanol [(+)-*p*IV] as a sigma receptor ligand and evaluated the potential of radioiodinated (+)-*p*IV for tumor imaging and therapy. (+)-[$^{125/131}$I]*p*IV was prepared by an iododestannylation reaction under no-carrier-added conditions with radiochemical purity over 99% after HPLC purification. Biodistribution experiments were performed by the intravenous injection of (+)-[^{125}I]*p*IV into mice bearing human prostate tumors (DU-145). Blocking studies were performed by intravenous injection of (+)-[^{125}I]*p*IV mixed with an excess amount of unlabeled sigma ligand into DU-145 tumor-bearing mice. For therapeutic study, (+)-[^{131}I]*p*IV was injected at a dose of 7.4 MBq followed by measurement of the tumor size. In biodistribution experiments, (+)-[^{125}I]*p*IV showed high uptake and long residence in the tumor. High tumor to blood and muscle ratios were achieved because the radioactivity levels of blood and muscle were low. However, the accumulations of radioactivity in non-target tissues, such as liver and kidney, were high. The radioactivity in the non-target tissues slowly decreased over time. Co-injection of (+)-[^{125}I]*p*IV with an excess amount of unlabeled sigma ligand resulted in a significant decrease in the tumor/blood ratio, indicating sigma receptor-mediated tumor uptake. In therapeutic study, tumor growth in mice treated with (+)-[^{131}I]*p*IV was significantly inhibited compared to that of an untreated group. These results indicate that radioiodinated (+)-*p*IV has a high potential for sigma receptor imaging in tumor and radionuclide receptor therapy. (*Cancer Sci* 2009; 100: 2188–2192)

It has been reported that there are at least two subtypes of sigma receptors, designated sigma-1 and sigma-2.[1] Whereas the sigma-1 receptor subtype has been cloned from various tissues and species,[2,3] the sigma-2 receptor subtype has not yet been cloned. The functions of sigma receptors have not yet been clearly defined. In the central nervous system, they have been shown to be involved in the regulation of neurotransmitter release, modulation of neurotransmitter receptor function, learning and memory processes, and regulation of movement and posture.[4] Although they are expressed in peripheral tissues such as liver, kidney, and endocrine organs, their function in these tissues has been much less understood. At the same time, it has been reported that both sigma receptor subtypes are highly expressed in a variety of human tumors such as prostate cancer, breast cancer, malignant melanoma, glioma, neuroblastoma, and non-small-cell lung carcinoma.[5,6] The high expression of sigma receptors in tumors suggests that they are appropriate targets for developing tumor-imaging agents. Furthermore, sigma receptors should be potential biomarkers of tumor proliferation because they are highly expressed in rapidly proliferating cells and are down-regulated when cells become quiescent.[7–9] For the time being, radiolabeled sigma ligands should be useful for monitoring the effects of chemotherapy at an early stage when morphologic changes are not observed.[10]

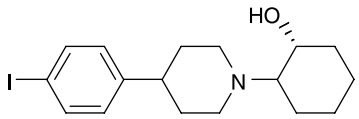

Fig. 1. Chemical structure of (+)-2-[4-(4-iodophenyl)piperidino] cyclohexanol [(+)-*p*IV].

Previously, we have developed several vesamicol analogs with iodine into the 4-phenylpiperidine moiety as sigma receptor imaging agents for investigating the central nervous system, and determined the binding affinities for the sigma receptors of the vesamicol analogs.[11,12] In these vesamicol analogs, the (+)-enantiomer of 2-[4-(4-iodophenyl)piperidino] cyclohexanol [(+)-*p*IV] (Fig. 1) showed the highest affinities for the receptors.[12] The inhibition constant (K_i) of (+)-*p*IV to sigma-1 and sigma-2 was 1.3 nM and 20.4 nM, respectively. The values mean that (+)-*p*IV has more than 10-times greater affinity for sigma-1 than that of (+)-pentazocine (Ki = 19.9 nM), which is known as a sigma-1 ligand, and the sigma-2 affinity of (+)-pIV is equivalent to that of 1,3-di(2-toyl)guanidine (DTG) (Ki = 22.5 nM), which is known as a non-selective sigma ligand.

In this study, to evaluate the potential of radioiodinated (+)-*p*IV for tumor imaging and receptor radionuclide therapy, we selected human DU-145 prostate cancer cells known to over-express sigma-1 and sigma-2 receptors[13] for preparation of tumor-bearing mice, and a biodistribution study, metabolite analysis, and therapeutic experiments were performed.

Materials and Methods

Chemicals. [^{125}I]Sodium iodide and [^{131}I]sodium iodide were purchased from Perkin Elmer (Waltham, MA, USA). TLC analyses were performed with silica plates (Art 5553; Merck, Darmstadt, Germany). (3,4-Dimethoxyphenethyl)-4-(3-phenylpropyl)piperazine (SA4503) was kindly supplied by M's Science (Kobe, Japan). Other reagents were of reagent grade and used as received.

Preparation of (+)-enantiomer of (+)-*p*IV. The (+)-enantiomer of *p*-iodovesamicol [(+)-*p*IV] was prepared using a method described previously.[14,15] Briefly, (+)-*p*IV was synthesized from the (+)-enantiomer of vesamicol, which was provided from racemic vesamicol by recrystallizing the diastereoisomeric salts using

[5]To whom correspondence should be addressed. E-mail: kogawa@p.kanazawa-u.ac.jp

doi: 10.1111/j.1349-7006.2009.01279.x

(–)-di-*p*-toluoyl-D-tartaric acid monohydrate, via a three-step reaction of nitration, amination, and iodination.

Preparation of (+)-[^{125}I]*p*IV and (+)-[^{131}I]*p*IV. (+)-[^{125}I]*p*IV and (+)-[^{131}I]*p*IV were prepared according to procedures described preciously with a slight modification.[16] Briefly, [^{125}I]sodium iodide solution (18.5 MBq/5 μL) or [^{131}I]sodium iodide solution (74 MBq/3 μL) was added to 5 μL of 3 M formic acid. (+)-2-[4-(4-Tributylstannyl)phenylpiperidino]cyclohexanol [(+)-*p*-tributylstannylvesamicol] (3 μg), synthesized as described previously,[17] in ethanol (3 μL) and 5 μL of 3% H_2O_2 was added and the reaction mixture was gently shaken. After 20 min of standing at room temperature, the reaction mixture was quenched with 3 μL of 10 M sodium hydroxide solution and then purified by reversed phase (RP)-HPLC performed with a Cosmosil $5C_{18}$-AR 300 column (4.6 × 150 mm; Nacalai Tesque, Kyoto, Japan) at a flow rate of 1 mL/min with a mixture of acetonitrile, water, and ethanolamine (75:25:0.05) as a mobile phase.

Biodistribution of (+)-[^{125}I]*p*IV in tumor-bearing mice. Experiments with animals were conducted in accordance with the Guidelines for the Care and Use of Laboratory Animals of Kanazawa University. The animals were housed with free access to food and water at 23°C with a 12-h alternating light/dark schedule. DU-145 cells were obtained from ATCC (Manassas, VA, USA) and grown in cell culture dishes in RPMI-1640 medium with phenol red, 10% heat-inactivated fetal calf serum, 100 μg/mL glutamine, 100 units/mL penicillin, and 100 μg/mL streptomycin. The cells were cultured in a humidified atmosphere of 95% air and 5% carbon dioxide at 37°C. They were then released from the dishes by treatment with 0.05% trypsin/EDTA. Next, the mice to be inoculated were anesthetized with pentobarbital. To produce tumors, approximately 5×10^6 of the prepared cells were injected subcutaneously into the right dorsum of 4-week-old-male BALB/c nude mice (15–19 g; Japan SLC, Hamamatsu, Japan). Biodistribution experiments were performed at approximately 14–21 days postinoculation, i.e. when tumors reached a palpable size. Groups of four or five mice were intravenously administered 100 μL of (+)-[^{125}I]*p*IV (37 kBq). At 1, 24, and 48 h postinjection, the mice were sacrificed. Tissues of interest were removed and weighed, and radioactivity counts were determined with an auto well gamma counter (ARC-380; Aloka, Tokyo, Japan) and corrected for background radiation.

Blocking studies. For blocking studies, the above-mentioned DU-145 tumor-bearing mice were intravenously administered 100 μL of (+)-[^{125}I]*p*IV (37 kBq) mixed with an excess of each unlabeled sigma ligand, haloperidol (10 μmol/kg), SA4503 (10 μmol/kg), or (+)-*p*IV (10 μmol/kg), respectively. At 1 h postinjection, the mice were sacrificed and biodistribution experiments were conducted as described above.

Metabolite analysis in blood, tumor, and other tissues. For metabolite analysis, the above-mentioned DU-145 tumor-bearing mice were intravenously administered 100 μL of (+)-[^{125}I]*p*IV (370 kBq). At 1 and 24 h postinjection, the mice were sacrificed. Blood was collected by heart puncture using a heparinized syringe, and tissues of interest were removed. The blood was centrifuged at 7000 *g* for 10 min at 4°C. After collecting the plasma, an equivalent volume of acetonitrile-water (1:1) was added to the plasma. The mixture was centrifuged at 7000 *g* for 10 min at 4°C. The tissues of interest (0.2–0.5 g) were homogenized in 1 mL of acetonitrile-water (1:1). Each homogenized sample was centrifuged at 7000 *g* for 10 min at 4°C. The supernatants were analyzed by TLC with ethyl acetate, hexane, and ethanolamine (3:7:0.1) as a developing solvent.

Determination of the partition coefficient. The partition coefficient of (+)-[^{125}I]*p*IV was measured as described previously with a slight modification.[18,19] Namely, (+)-[^{125}I]*p*IV was mixed with 3 mL each of 1-octanol and phosphate buffer (0.02 M, pH 7.4) in a test tube. The mixture was vortexed for 10 min. After vortex, the mixture was centrifuged at 1000 *g* for 5 min. 2.5 mL of 1-octanol was removed and added to 2.5 mL of new phosphate buffer (0.02 M, pH 7.4). After repeating the same procedure twice, 100 μL and 1 mL of 1-octanol and phosphate buffer were taken and their radioactivity and weight were measured. The partition coefficient was determined by calculating the ratio of cpm/mL in 1-octanol to that in the buffer, and expressed as a common logarithm (log *P*).

Therapy. The mice were randomly distributed in the experimental groups. When the tumors had reached a palpable size, (+)-[^{131}I]*p*IV was injected intravenously at a dose of 7.4 MBq. A group of untreated mice served as a control group. After injection, tumor size was measured with a slide caliper in two dimensions, and mouse weights were measured 2–3 times per week. Individual tumor volumes (V) were calculated by the formula $V = [\text{length} \times (\text{width})^2]/2$ and compared to the values on the day of treatment (relative tumor volume).

Statistical evaluation. An unpaired Student's *t*-test was used for the therapeutic experiments. One-way ANOVA followed by Dunnett's post-hoc test compared to the control group was used for experiments in the blocking study. Results were considered statistically significant at $P < 0.05$.

Results

Preparation of (+)-[^{125}I]*p*IV. (+)-[^{125}I]*p*IV and (+)-[^{131}I]*p*IV were prepared by the iododestannylation reaction under no-carrier-added conditions with high radiochemical yield (87% and 83%, respectively). After purification by RP-HPLC, (+)-[^{125}I]*p*IV and (+)-[^{131}I]*p*IV showed radiochemical purities of over 99%.

Biodistribution experiments of (+)-[^{125}I]*p*IV in tumor-bearing mice. Table 1 lists the biodistribution of (+)-[^{125}I]*p*IV in DU-145 tumor-bearing mice. (+)-[^{125}I]*p*IV showed high uptake and long retention in the tumors. Since the radioactivity levels in blood and muscle were low, high tumor to blood and muscle ratios were achieved. However, the accumulation of radioactivity in abdominal organs such as liver and kidney was high. The clearance of radioactivity in these organs was faster than that in the tumor. At the same time, the accumulation of (+)-[^{125}I]*p*IV in the stomach was low, indicating that deiodination was not observed *in vivo*.

Blocking studies. The effects of some sigma ligands on tumor uptake of (+)-[^{125}I]*p*IV at 1 h postinjection are shown as % injected dose per gram in tumor in Figure 2. Co-injection of an excess amount of haloperidol, SA4503, or (+)-*p*IV resulted in a significant decrease in tumor uptake after injection of (+)-[^{125}I]*p*IV.

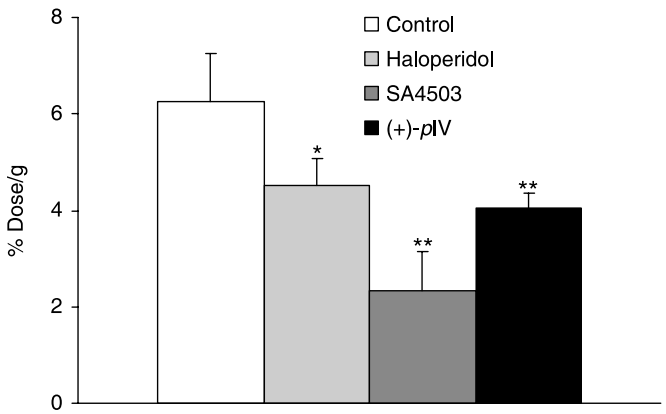

Fig. 2. Comparison of tumor uptake (mean ± SD) of (+)-[^{125}I]*p*IV at 1 h postinjection under no-carrier-added conditions and under co-injection of haloperidol, SA4503, or (+)-2-[4-(4-iodophenyl)piperidino] cyclohexanol [(+)-*p*IV]. Significance was determined using one-way ANOVA followed by Dunnett's post-hoc test (*$P < 0.05$, **$P < 0.01$ vs. control).

Table 1. Biodistribution of radioactivity after intravenous injection of (+)-[^{125}I]*p*IV in tumor-bearing mice

Tissue	Time after injection		
	1 h	24 h	48 h
Blood	0.24	0.71	0.37
	(0.03)	(0.05)	(0.06)
Tumor	6.27	8.78	6.04
	(1.00)	(0.41)	(1.19)
Liver	16.91	15.23	5.24
	(0.79)	(0.62)	(0.41)
Kidney	16.24	9.38	4.21
	(2.52)	(0.60)	(0.28)
Intestine	6.44	4.89	1.50
	(1.10)	(0.16)	(0.19)
Spleen	13.62	4.04	1.75
	(2.73)	(0.53)	(0.25)
Lung	15.62	3.83	1.81
	(5.87)	(0.44)	(0.62)
Heart	8.21	1.62	0.65
	(1.85)	(0.21)	(0.07)
Stomach†	0.66	0.59	0.27
	(0.09)	(0.05)	(0.05)
Brain	7.65	2.89	1.08
	(2.15)	(0.10)	(0.09)
Muscle	2.41	0.64	0.30
	(0.77)	(0.17)	(0.09)
T/B ratio	26.20	12.39	16.48
	(4.23)	(0.98)	(2.16)
T/M ratio	2.72	14.30	20.54
	(0.55)	(2.76)	(2.02)

Data are expressed as % injected dose per gram tissue. Each value represents the mean (SD) for four or five animals.
†Data are expressed as % injected dose.
T/B ratio, tumor : blood ratio; T/M ratio, tumor : muscle ratio.

Table 2. Analysis of metabolites after intravenous injection of (+)-[^{125}I]*p*IV in tumor-bearing mice

Tissue	Time after injection	
	1 h	24 h
Blood	3.7	1.4
	(2.6)	(1.5)
Tumor	83.1	40.7
	(6.0)	(2.8)
Liver	76.0	10.4
	(5.3)	(2.2)
Kidney	86.5	8.7
	(5.5)	(2.0)
Lung	86.2	10.8
	(4.0)	(0.8)
Brain	94.8	22.8
	(2.6)	(1.3)

Data are expressed as % of intact (+)-[^{125}I]*p*IV. Each value represents the mean (SD) for three samples.

Metabolite analysis in blood, tumor, and other tissues. Table 2 lists the results of the metabolite analyses after intravenous injection of (+)-[^{125}I]*p*IV in DU-145 tumor-bearing mice. At 1 h postinjection, large proportions of radioactivity existed as an intact form in almost all tissues except blood. In contrast, at 24 h postinjection, the proportions of the intact form in all tissues were much lower than those at 1 h postinjection. At 24 h postinjection, radioactivity in the tumor showed a relatively large proportion of the intact form (40.7%) compared with those in other tissues. In blood, almost no intact (+)-[^{125}I]*p*IV was observed at 1 and 24 h postinjection (3.7% and 1.4%, respectively).

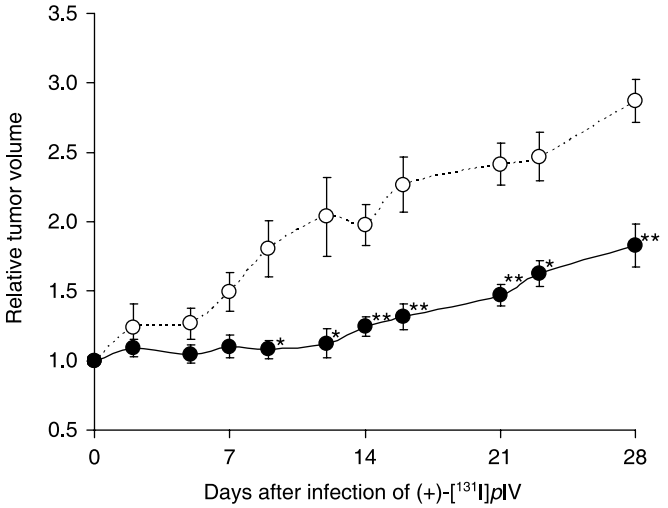

Fig. 3. Curves depicting inhibition of growth of DU-145 on therapy with (+)-[^{131}I]*p*IV (closed circles) compared with no treatment (open circles). Data are expressed as tumor volume relative to that on the day of treatment (mean ± SEM for four mice). Significance was determined using the Student's *t*-test (*$P < 0.05$, **$P < 0.01$ vs. untreated group).

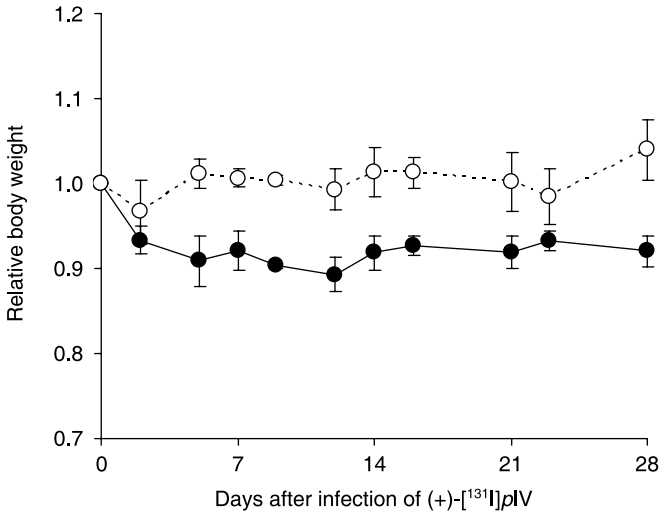

Fig. 4. Body weight of DU-145 tumor-bearing mice treated with (+)-[^{131}I]*p*IV (closed circles) or with no treatment (open circles). Data are expressed as relative value to initial body weight (mean ± SEM for four mice).

Determination of the partition coefficient. The log *P*-value of (+)-[^{125}I]*p*IV was 2.08 ± 0.02 (mean ± SD for four samples).

Therapy. The volume of the tumors as a function of time is shown in Figure 3. As can be seen, tumor growth in the mice treated with (+)-[^{131}I]*p*IV was significantly inhibited compared to that of the untreated group. Weight could be used as a marker for the general health of the mice (Fig. 4). The mice treated with (+)-[^{131}I]*p*IV lost weight, which was probably caused by treatment-related toxicity, but the weight loss was less than 10% of their starting body weight.

doi: 10.1111/j.1349-7006.2009.01279.x

Discussion

In the case of the differential diagnosis of tumors, information obtained from Single photon emission computed tomography (SPECT) or PET imaging should be more important than that from other imaging modalities such as CT, MRI, or ultrasound. That is to say, among those imaging modalities, nuclear medicine modality is most advantageous for detecting functional changes such as changes of receptor density, metabolism, and so on. It has been reported that the density of sigma receptors affects the condition of tumors.[7,20] Therefore, nuclear imaging agents for sigma receptors could be useful in the differential diagnosis of tumors.[9] In this study, we first examined the potential of radioiodine-labeled (+)-*p*IV, which has a very high affinity for sigma receptors, as a tumor-imaging agent.

In the biodistribution experiments in the tumor-bearing mice, (+)-[^{125}I]*p*IV showed a high uptake of radioactivity in the DU-145 tumor as we expected. Tu *et al*. described that not only receptor affinity but also optimal lipophilicity is important in the design of receptor-based tumor-imaging agents.[21] The measured partition coefficient (log *P*) for (+)-[^{125}I]*p*IV was 2.08. The value was much less than what we expected because the calculated log *P*-value for *p*IV was 4.45 using CS ChemDraw Ultra software (Cambridge Soft, Cambridge, MA, USA). A slight contamination or the presence of hydrophilic impurities could underestimate the log *P*-value. Then, it might be difficult to accurately determine the log *P*-value for a high lipophilicity radioactive compound via the shake-flask method. Although it is not clear whether the lipophilicity of (+)-*p*IV is optimal for tumor uptake, part of the high uptake in tumors might be derived from the appropriate lipophilicity of (+)-[^{125}I]*p*IV. Additionally, since (+)-[^{125}I]*p*IV showed low radioactivity in blood and muscle, high tumor to blood and muscle ratios were achieved (Table 1). In order to determine *in vivo* binding of (+)-[^{125}I]*p*IV to sigma receptors, (+)-[^{125}I]*p*IV was co-injected with excess amounts of some types of sigma ligands. The co-injection significantly decreased tumor uptake of radioactivity (Fig. 2), which indicates the receptor specificity of (+)-[^{125}I]*p*IV uptake in DU-145 tumors *in vivo*. These results indicate that (+)-*p*IV labeled with I-123 and I-124 instead of I-125 as a radionuclide could be useful as sigma receptor-imaging agents in tumors for SPECT and PET, respectively. Meanwhile, from our previous *in vitro* experiments,[12] we assume that (+)-[^{125}I]*p*IV prefers sigma-1, but could bind to not only sigma-1 but also sigma-2. Sigma-1 and sigma-2 receptors are highly expressed in DU-145 cells.[13] In this study, SA4503 inhibited tumor uptake of (+)-[^{125}I]*p*IV more strongly than with haloperidol. SA4503 binds mainly to sigma-1, and haloperidol is a non-selective sigma ligand.[22] Therefore, the results from the *in vivo* experiments in this study suggest that (+)-[^{125}I]*p*IV binds to sigma-1 receptors, but it is not clear whether (+)-[^{125}I]*p*IV also binds to sigma-2 receptors.

The problem of the tracer was high accumulations of radioactivity in non-target tissues, such as liver and kidney. As described in the introduction section, since sigma receptors are expressed in not only tumor but also non-target tissues such as in the liver and kidney, some parts of the accumulation of the radioactivity in non-target tissues should be sigma receptor–specific. It may be difficult to avoid some uptakes in non-target tissues for labeled sigma ligands. Tu *et al*. mentioned that sigma-1-selective or sigma-1/sigma-2-non-selective compounds might not be ideal candidates for imaging tumors because many kinds of tumors possess a higher density of sigma-2 receptors than the surrounding normal tissue. On the other hand, the density of sigma-1 receptors in tumor cells is generally less than that present in normal tissues.[21] Although it was reported that rat liver and kidney contain high densities of sigma-1 and sigma-2 receptors with sigma-2 sites comprising 75–80% of the total sigma receptors population,[23] Mach *et al*. performed biodistribution experiments with a ^{18}F-labeled compound possessing a high affinity for both sigma-1 and sigma-2 receptors with co-injection of the unlabeled sigma-1 selective ligand and showed that the blocking of sigma-1 receptors reduced the accumulation of radioactivity in non-target tissues except liver.[24] Their studies indicate that labeled specific sigma-2 ligands could show less accumulation in non-target tissues compared with sigma-1-specific or non-selective ligands. At the same time, lipophilicity might affect not only tumor uptake but also non-target tissue uptake and higher lipophilicity might lead to high non-specific uptake in both target and non-target tissues.[25,26] Some parts of the accumulation of (+)-[^{125}I]*p*IV in non-target tissues, especially in liver, should be derived from its lipophilicity. Although the radioactivity in the non-target tissues gradually decreased compared to that in tumor, the clearance of the radioactivity in the non-target tissues was not fast. Consequently, it most likely interferes with the acquisition of clear images at early times after injection of radioiodine-labeled (+)-*p*IV.

In the metabolite studies, the clearance of the intact (+)-[^{125}I]*p*IV in tumors was slower than that in any other organ (Table 2). When we calculated (% injected dose per gram) $\times$ (ratio of intact (+)-[^{125}I]*p*IV) at 24 h postinjection of (+)-[^{125}I]*p*IV, the values for blood, tumor, liver, kidney, lung, and brain were 0.01, 3.57, 1.58, 0.82, 0.42, and 0.66, respectively. Much more intact (+)-[^{125}I]*p*IV remained in tumors compared with that in other organs. Whether these results were caused by differences of metabolic rate is not clear from our data. Even if more intact (+)-[^{125}I]*p*IV in tumors is caused by a slow metabolic rate, further studies would be needed to elucidate the causes. However, more intact (+)-[^{125}I]*p*IV should affect the more prolonged residence in tumors than that in other organs. Actually, previous studies have reported that the clearance of the sigma ligands from the brain was faster than those from tumors.[13,24,27,28] The long residence of radiotracer in tumors is convenient for internal radiotherapy. Accordingly, we supposed that radioiodinated (+)-*p*IV could also be used as an internal radionuclide therapy by using I-131, which emits middle energy of beta particles for therapy, instead of I-125. We examined the potential of (+)-[^{131}I]*p*IV as a therapeutic agent. As a result, a single treatment with (+)-[^{131}I]*p*IV (7.4 MBq/mice) achieved significant inhibition of tumor growth in tumor-bearing mice compared with a control group (Fig. 3). As far as we know, this was the first trial to use a radiolabeled sigma ligand for receptor radionuclide therapy. Although the data are insufficient, these results indicate that (+)-[^{131}I]*p*IV has potential as an agent for radionuclide receptor therapy.

In conclusion, radioiodinated (+)-*p*IV has a high potential for sigma receptor imaging in tumor and radionuclide receptor therapy because of its high tumor uptake via sigma receptor in an animal model. However, further studies are needed in order to reduce the radioactivity levels in non-target tissues.

Acknowledgment

This work was supported in part by Grants-in-Aid for Scientific Research from the Ministry of Education, Culture, Sports, Science and Technology of Japan.

References

1 Quirion R, Bowen WD, Itzhak Y *et al*. A proposal for the classification of sigma binding sites. *Trends Pharmacol Sci* 1992; **13**: 85–6.

2 Hanner M, Moebius FF, Flandorfer A *et al*. Purification, molecular cloning, and expression of the mammalian sigma1-binding site. *Proc Natl Acad Sci USA* 1996; **93**: 8072–7.

3 Kekuda R, Prasad PD, Fei YJ, Leibach FH, Ganapathy V. Cloning and

functional expression of the human type 1 sigma receptor (hSigmaR1). *Biochem Biophys Res Commun* 1996; **229**: 553–8.
4 Su TP. Delineating biochemical and functional properties of sigma receptors: emerging concepts. *Crit Rev Neurobiol* 1993; **7**: 187–203.
5 Vilner BJ, John CS, Bowen WD. Sigma-1 and sigma-2 receptors are expressed in a wide variety of human and rodent tumor cell lines. *Cancer Res* 1995; **55**: 408–13.
6 Bem WT, Thomas GE, Mamone JY *et al*. Overexpression of sigma receptors in nonneural human tumors. *Cancer Res* 1991; **51**: 6558–62.
7 Mach RH, Smith CR, al-Nabulsi I, Whirrett BR, Childers SR, Wheeler KT. Sigma 2 receptors as potential biomarkers of proliferation in breast cancer. *Cancer Res* 1997; **57**: 156–61.
8 Wheeler KT, Wang LM, Wallen CA *et al*. Sigma-2 receptors as a biomarker of proliferation in solid tumours. *Br J Cancer* 2000; **82**: 1223–32.
9 Hirata M, Mori T, Umeda T, Abe T, Yamamoto T, Ohmomo Y. Evaluation of radioiodinated 1-[2-(3,4-Dimethoxyphenyl) ethyl]-4-(2-iodophenylpropyl) piperazine as a tumor diagnostic agent with functional sigma receptor imaging by single photon emission computed tomography. *Biol Pharm Bull* 2008; **31**: 879–83.
10 van Waarde A, Shiba K, de Jong JR, Ishiwata K, Dierckx RA, Elsinga PH. Rapid reduction of sigma1-receptor binding and ^{18}F-FDG uptake in rat gliomas after in vivo treatment with doxorubicin. *J Nucl Med* 2007; **48**: 1320–6.
11 Shiba K, Yano T, Sato W, Mori H, Tonami N. Characterization of radioiodinated (-)-ortho-iodovesamicol binding in rat brain preparations. *Life Sci* 2002; **71**: 1591–8.
12 Shiba K, Ogawa K, Mori H. In vitro characterization of radioiodinated (+)-2-[4-(4-iodophenyl) piperidino]cyclohexanol [(+)-pIV] as a sigma-1 receptor ligand. *Bioorg Med Chem* 2005; **13**: 1095–9.
13 John CS, Vilner BJ, Geyer BC, Moody T, Bowen WD. Targeting sigma receptor-binding benzamides as in vivo diagnostic and therapeutic agents for human prostate tumors. *Cancer Res* 1999; **59**: 4578–83.
14 Shiba K, Mori H, Matsuda H *et al*. Synthesis of radioiodinated analogs of 2-(4-phenylpiperidino) cyclohexanol (vesamicol) as vesamicol-like agent. *Nucl Med Biol* 1995; **22**: 205–10.
15 Rogers GA, Parsons SM, Anderson DC *et al*. Synthesis, in vitro acetylcholine-storage-blocking activities, and biological properties of derivatives and analogues of trans-2-(4-phenylpiperidino) cyclohexanol (vesamicol). *J Med Chem* 1989; **32**: 1217–30.
16 Akhter N, Shiba K, Ogawa K *et al*. A change of in vivo characteristics depending on specific activity of radioiodinated (+)-2-[4-(4-iodophenyl) piperidino]cyclohexanol [(+)-pIV] as a ligand for sigma receptor imaging. *Nucl Med Biol* 2008; **35**: 29–34.
17 Shiba K, Ogawa K, Ishiwata K, Yajima K, Mori H. Synthesis and binding affinities of methylvesamicol analogs for the acetylcholine transporter and sigma receptor. *Bioorg Med Chem* 2006; **14**: 2620–6.
18 Wilson AA, Jin L, Garcia A, DaSilva JN, Houle S. An admonition when measuring the lipophilicity of radiotracers using counting techniques. *Appl Radiat Isot* 2001; **54**: 203–8.
19 Ogawa K, Mukai T, Arano Y *et al*. Rhenium-186-monoaminemonoamidedithiol-conjugated bisphosphonate derivatives for bone pain palliation. *Nucl Med Biol* 2006; **33**: 513–20.
20 Aydar E, Onganer P, Perrett R, Djamgoz MB, Palmer CP. The expression and functional characterization of sigma 1 receptors in breast cancer cell lines. *Cancer Lett* 2006; **242**: 245–57.
21 Tu Z, Dence CS, Ponde DE *et al*. Carbon-11 labeled sigma 2 receptor ligands for imaging breast cancer. *Nucl Med Biol* 2005; **32**: 423–30.
22 Hashimoto K, Ishiwata K. Sigma receptor ligands: possible application as therapeutic drugs and as radiopharmaceuticals. *Curr Pharm Des* 2006; **12**: 3857–76.
23 Hellewell SB, Bruce A, Feinstein G, Orringer J, Williams W, Bowen WD. Rat liver and kidney contain high densities of sigma 1 and sigma 2 receptors: characterization by ligand binding and photoaffinity labeling. *Eur J Pharmacol* 1994; **268**: 9–18.
24 Mach RH, Huang Y, Buchheimer N *et al*. [^{18}F]N-4′-fluorobenzyl-4-(3-bromophenyl) acetamide for imaging the sigma receptor status of tumors: comparison with [^{18}F]FDG, and [^{125}I]IUDR. *Nucl Med Biol* 2001; **28**: 451–8.
25 Garg S, Kothari K, Thopate SR, Doke AK, Garg PK. Design, synthesis, and preliminary in vitro and in vivo evaluation of N-(2-diethylaminoethyl)-4-[^{18}F]fluorobenzamide ([^{18}F]-DAFBA): a novel potential PET probe to image melanoma tumors. *Bioconjug Chem* 2009.
26 Brandau W, Niehoff T, Pulawski P *et al*. Structure distribution relationship of iodine-123-iodobenzamides as tracers for the detection of melanotic melanoma. *J Nucl Med* 1996; **37**: 1865–71.
27 Kawamura K, Kubota K, Kobayashi T *et al*. Evaluation of [^{11}C]SA5845 and [^{11}C]SA4503 for imaging of sigma receptors in tumors by animal PET. *Ann Nucl Med* 2005; **19**: 701–9.
28 Waterhouse RN, Collier TL. In vivo evaluation of [^{18}F]1-(3-fluoropropyl)-4-(4-cyanophenoxymethyl) piperidine: a selective sigma-1 receptor radioligand for PET. *Nucl Med Biol* 1997; **24**: 127–34.

doi: 10.1111/j.1349-7006.2009.01279.x